Solving the radius and position of a passing charged sphere using a coaxial probe

Janne Peltonen, Matti Murtomaa, Jarno Salonen
Dept. of Physics and Astronomy
University of Turku, Finland
e-mail: janne.m.peltonen@utu.fi

***Abstract*— As a charged object passes a grounded metal probe, a bipolar current signal is induced. By integrating the signal over time, the induced charge as a function of time can be obtained. The shape of the signal depends on the size, distance both in *x* and *y* directions, speed, and charge of the object, and also on the geometry of the probe. Coaxial induction probe with a vertically split outer sensor was previously simulated and built to determine the aforementioned properties of charged spheres but only if their velocity was known. It was verified that the simulation data matched with the ones of the experiments. In this research, the probe was calibrated to solve the radius and distance of the passing objects using simulations in such a way that the velocity of the object could be determined later. Solving the radius and distance accurately is inevitable in order to determine the charge and velocity from other equations at later stages. The solutions were rather accurate as the distance was small but, on the other hand, in some situations these equations gave several roots, one of which was the correct one. Choosing the correct root was not always possible, which narrowed the range of use of the measurement system. However, the distance measured from the center of the sphere could be determined rather easily but with no information about the radius. In these cases, the charge density could not be calculated since the size of the object remained unknown.**

I. Introduction

Charge-to-mass ratio *Q/m* is among the most important parameters when dealing with electrostatic charging of powders. Powder particles are triboelectrically charged by frictional contacts between surfaces and other particles [1]. The amount of charge that is accumulated on the particles depends greatly on the surface conditions of the material and on the environmental conditions, mainly humidity. The simplest method for estimating this value is to measure the charge by inserting a sample of powder into a Faraday cup and then weighing it. However, additional charge may be produced if the sample, for example, makes contact with a surface before it enters the cup [2][3]. This method has been used in powder transport and in fluidized beds [4][5]. However, if a sample is inserted into the cup, the measured result may not completely match with the real on-line situation where the powder is in motion. Moreover, the described measurement procedure is very slow and is not useful in on-line measurements. Therefore, another kind of reliable measurement system is needed.

In on-line measurements, induction probes are often used [6]. The probe must be con-

ductive. As a charged object passes a grounded probe, a bipolar current signal is induced and can be measured [7]. If the signal is integrated over time, the induced charge as a function of time is obtained. The shape of the signal is affected by the charge (Q), speed (v), radius (r), passing distance (x, y) of the object, and by the geometry of the probe. Often only the charge can be determined.

In previous studies, a coaxial induction probe to measure these object properties was presented [8]–[10]. The first version consisted of a circular inner sensor and a ring-shaped outer sensor [8][9]. The improved version had the outer ring sensor made of two adjacent parts in order to measure objects which passed the probe asymmetrically, *i.e.* the sphere trajectories were displaced from the probe axis [10]. Also, the radius of the outer sensor was increased in order to increase sensitivity [11]. The probe was attached into the wall of a metal tube so that its curvature matched with one of the tube. Charged spheres were set to pass the probe vertically. The induced current signals were integrated over time. Gaussian curves were fitted to the integrals, and the amplitudes (A_o and A_i for outer and inner sensor) and widths (W_o and W_i) of the curves were collected. Also, the amplitude ratio A_o/A_i and width ratio W_o/W_i were calculated. For the improved version, also the amplitudes A_L and A_R (for left and right part of the outer ring) and their ratio were recorded.

Experimental measurements were done with spheres of different sizes, passing distances, and charges. Calibration equations were determined from the data. The ratios A_o/A_i and W_o/W_i were functions of only the radius and distance of the object. However, in the previous studies, width ratio data could not be used because of significant standard deviation. Instead, the data for width W_o was used together with A_o/A_i to calculate the radius and distance. Unfortunately, since the width of the signal was also function of the speed, the speed of the sphere had to be known. The charge was calculated from A_o.

Recent computer simulations with FEM software COMSOL Multiphysics showed that the experimental measurements matched with simulation data. It was also evident that the somewhat significant error limits in experiments were not only caused by inhomogeneous charging of the spheres but also by imperfections in determining the passing distance both in x and y direction. From this reason, instead of using experimental data, simulation data was used in calibrations in the present study. Solving the radius and distance is the important first step in this process and is discussed in more detail in this paper. Calculating the radius of the sphere correctly is of great important when calculating the charge-to-mass or charge-to-volume ratio, since the volume is proportional to r^3.

II. Methods

The simulations were done using COMSOL Multiphysics. A coaxial probe with a vertically split outer ring was perpendicularly attached to a grounded metal pipe (inner radius R = 50.000 mm). The radius of the inner and outer sensor was 2.000 mm and 10.000 mm, respectively. The thickness of the outer sensor was 2.000 mm and it was divided into two adjacent parts with 1.000 mm thick insulators. Charged spheres were set to pass the probe in z-direction. The radius was varied from 7.500 mm to 20.000 mm, passing distance in x direction (perpendicular distance from the edge of the sphere) from 1.000 mm to 30.000 mm and in y direction (displacement from the probe axis) from 0.000 mm to 8.000 mm. Induced charge was calculated by integrating the surface charge density over

the surface of the sensors. The probe geometry and the measurement set-up are presented in Fig. 1.

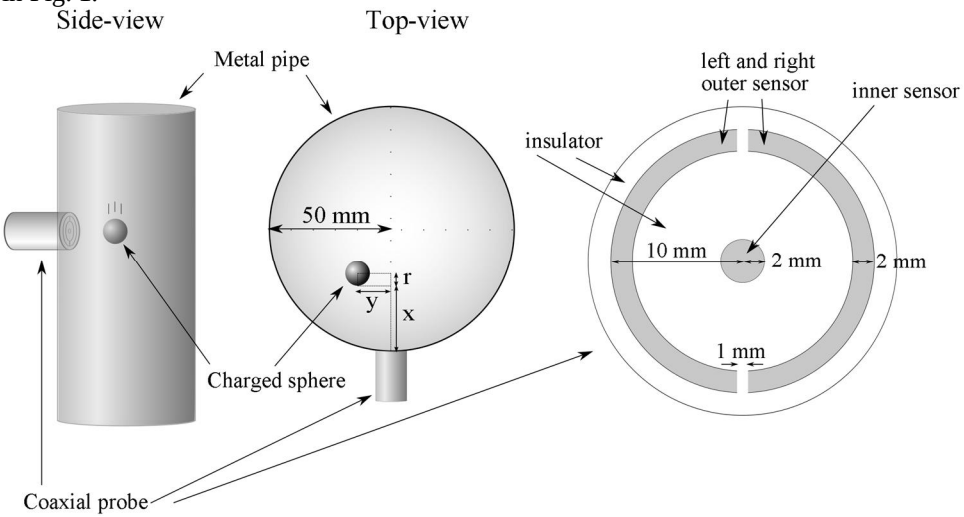

Fig. 1 Side-view (left) and top-view (center) from the set-up, and the tip of the coaxial probe (right).

Unlike in previous studies, pseudo-Voigt functions were fitted to the integrated data instead of Gaussian curves since they fitted much better. The Voigt profile is a convolution of Gaussian and Lorentzian profile. However, pseudo-Voigt function is a linear combination of these two profiles and has a lower computational expense than the original Voigt function. Mathematically pseudo-Voigt profile is expressed as a function of object's position in *z*-direction

$$A(z) = A_0 + S\left[m\frac{2}{\pi}\frac{W}{4(z-z_c)^2+W^2} + (1-m)\frac{\sqrt{4\ln 2}}{\sqrt{\pi}W}e^{-\frac{4\ln 2}{W^2}(z-z_c)^2}\right] \quad (1)$$

where W is the full width at half maximum, z_c is the center, S is the area, m is the profile shape factor and A_0 is the offset. The amplitude A can be observed as the value of the function at point z_c:

$$A = A_0 + S\left[m\frac{2}{\pi W} + (1-m)\frac{\sqrt{4\ln 2}}{\sqrt{\pi}W}\right]. \quad (2)$$

III. Results and Discussion

A. Calibration equations

The experimentally measured data matched with the simulated data. Therefore, the calibration was determined using the simulated data. The amplitudes A and widths W of the fitted curves were collected, and it was noticed that A_L/A_R, A_R/A_i and $(W_R+W_L)/W_i$ were the most suitable ratios to form the calibration equations. The ratio A_L/A_R was used to detect spheres that passed the probe symmetrically: for a symmetrically passing object, *i.e.* for an object for which the distance in y direction was $y = 0$, the ratio was exactly $A_L/A_R = 1$. The ratios A_R/A_i and $(W_R+W_L)/W_i$ decreased exponentially when either x or r

was increased. Calibration equations $A_R/A_i(r, x, y)$, $A_L/A_R(r, x, y)$ and $(W_R+W_L)/W_i(r, x, y)$ were formed in order to solve x, y and r.

The equations were determined using mathematical software called Eureqa Desktop (Nutonian, Inc.). Eureqa used symbolic regression to determine approximate equations that would describe the inserted simulation data. The software was set to seek solutions of form

$$f(r,x,y) = f_1(r,y)\exp\left(-\frac{x}{f_2(r,y)}\right) + f_3(r,y)\exp\left(-\frac{x}{f_4(r,y)}\right) + f_0 \qquad (3)$$

by minimizing the squared error of the fit. As equation building blocks, the program was allowed to use constants, input variables (r, x and y), additions, subtractions, multiplications, divisions, and exponential functions.

B. Solving the equations

The formed equations were solved with LabVIEW (National Instruments) using a built-in non-linear solver. The number of roots varied from zero to five. Roots were automatically neglected if the values were negative or, based on geometry, if they did not fulfill the condition

$$\sqrt{y^2 + (R - x - r)^2} + r < R \qquad (4)$$

as otherwise the sphere would have been outside the pipe. For up to approximately x = 10 mm one of the roots was close to the known solution. However, the others were possible solutions as well. For x > 10 mm the accuracy got worse and the real solution was nowhere to be found due to imperfections in the equations. At larger distances, A_L/A_R, A_R/A_i and $(W_R+W_L)/W_i$ approached the same value for each radius and therefore small variations in measured parameters caused significant differences in calculated solutions. The increase in radius influenced the shape of the signal similarly as did the increase in distance. Therefore, it was hard to specify whether the signal was caused by a big object near the probe or a smaller object further away.

From these reasons, the range of use of the probe had to be narrowed. The maximum calculated values of x and y were set to 6 mm. Otherwise the root was neglected. If two or more roots had distance smaller than 6 mm, all the roots were neglected. In cases were the roots were close enough to each other (radii within ~1.5 mm), average value was considered as a good approximation. In most cases, this method provided good results. In Fig. 2 a), b) and c) are presented averages and standard deviations of the calculated values. The distance in y-direction (displacement) matched well with the real values. Moreover, standard deviations were small. The averages of the radii had larger error limits especially with smaller spheres. Nevertheless, the points were close to the one-to-one line. The weakest performance was obtained when the distance in x-direction (perpendicular distance) was calculated. Despite restricting calculated distance values in both x- and y-direction to 6 mm at maximum, there were some situations where the distance in x-direction was in reality larger than 6 mm. Therefore, the data points started to deviate from the real values. This was obviously a major cause of error in the calculated radii in Fig. 2 b).

As seen in Fig. 2 d), if the distance from the center of the sphere was calculated, the values were close to real ones. This might be useful information in some applications.

However, the charge-to-volume or charge-to-mass ratio cannot be calculated if the radius is not known.

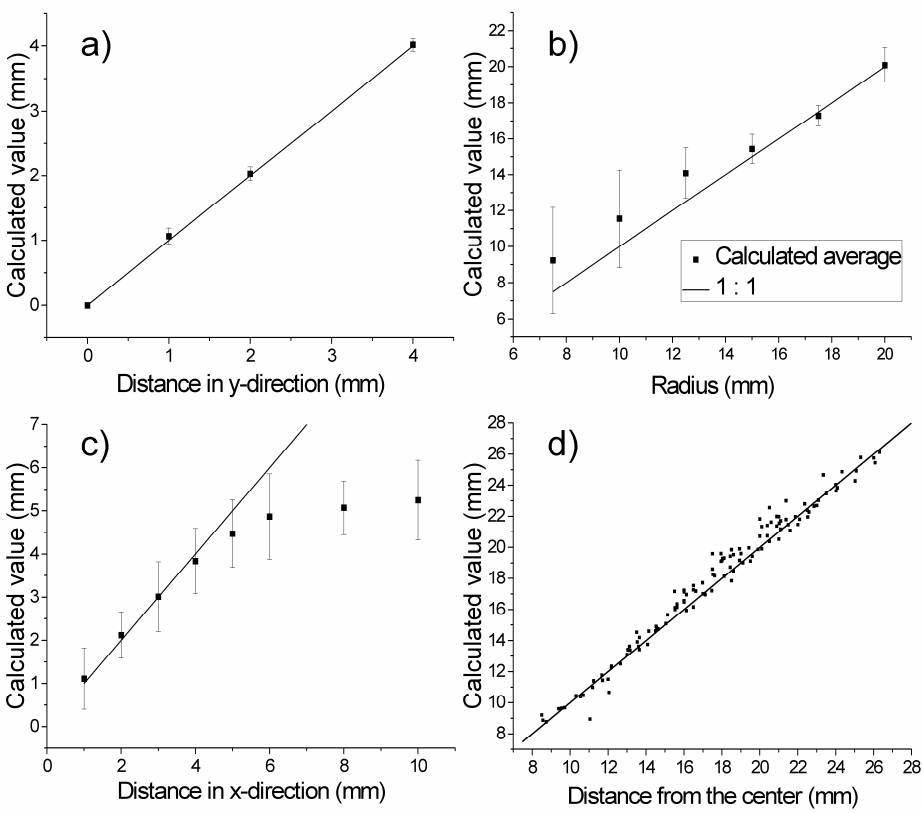

Fig. 2 Calculated averages of a) distance in *y*-direction, b) radius, c) distance in *x*-direction, and d) distance from the center of the sphere (individual data points).

IV. Conclusion

With the coaxial induction probe, solving the radius and distance is necessary in order to calculate the charge density of a passing object or the powder in case of a bubbling fluidized bed. Because increasing the radius affects in a rather similar way as does increasing the distance from the probe, with larger distances it is hard to differentiate which part of the broadening of the signal arises from the radius. From this reason, the distances both in *x*- and *y*-directions were limited up to 6 mm. The distance measured from the center of the passing object could be calculated easily, but without information about the radius and thus with no information about the charge density.

Acknowledgments

Authors are grateful to University of Turku Graduate School (UTUGS-PCS) for financing the study.

REFERENCES

[1] S. Matsusaka, H. Maruyama, T. Matsuyama, and M. Ghadiri, "Triboelectric charging of powders: A review," *Chem. Eng. Sci.*, vol. 65, no. 22, pp. 5781–5807, 2010.

[2] J. A. Cross, *Electrostatics: Principles, problems and applications*. Bristol: IOP Publishing Limited, 1987.

[3] P. Mehrani, H. T. Bi, and J. R. Grace, "Electrostatic charge generation in gas-solid fluidized beds," *J. Electrostat.*, vol. 63, no. 2, pp. 165–173, Feb. 2005.

[4] M. Murtomaa, J. Peltonen, and J. Salonen, "One-step measurements of powder resistivity as a function of relative humidity and its effect on charging," *J. Electrostat.*, vol. 76, pp. 78–82, 2015.

[5] K. Choi, T. Mogami, T. Suzuki, and M. Yamaguma, "A novel bipolar electrostatic ionizer for charged polypropylene granules used in a pneumatic powder transport facility," *J. Loss Prev. Process Ind.*, vol. 40, pp. 502–506, 2016.

[6] D. Boland and D. Geldart, "Electrostatic charging in gas fluidised beds," *Powder Technol.*, vol. 5, no. 5, pp. 289–297, 1972.

[7] M. Machida and B. Scarlett, "Development of Displacement Current Tomography System," *Part. Part. Syst. Charact.*, vol. 15, no. September 1997, pp. 36–41, 1998.

[8] M. Murtomaa and J. Salonen, "Simultaneous measurement of particle charge, distance and size using coaxial induction probe," *J. Phys. Conf. Ser.*, vol. 646, no. 012038, 2015.

[9] J. Peltonen, M. Murtomaa, and J. Salonen, "A coaxial induction probe for measuring the charge, size and distance of a passing object," *J. Electrostat.*, vol. 77, pp. 94–100, Oct. 2015.

[10] J. Peltonen, M. Murtomaa, A. Saikkonen, and J. Salonen, "A coaxial probe with a vertically split outer sensor for charge and dimensional measurement of a passing object," *Sens. Actuat. A*, vol. 244, pp. 44–49, 2016.

[11] J. Peltonen, M. Murtomaa, and J. Salonen, "Simulating a coaxial induction probe for measuring the charge, size and distance of a passing object," in *Proc. ESA Annual Meeting on Electrostatics*, 2015.